Egypt. J. Chem. **Vol. 62**, No.1 pp. 141 - 148 (2019)

Novel Photosynthesis of CeO_2 Nanoparticles from Its Salt with Structural and Spectral Study

Zaid Hamid Mahmoud*, Omaima Emad Khalaf, Mohammed Alwan Farhan
Department of Chemistry, College of Science, Diyala University, Iraq.

THE NANOPARTICLES of cerium oxide were synthesized using the novel photolysis method. The nanoparticles characterized by X-ray diffraction (XRD), UV-Visible spectroscope (UV-Vis), transmission electron microscope (TEM), scanning electron microscope (SEM), Raman spectroscopy, X-ray photoelectron spectroscopy (XPS) and Photoluminescence spectrum (PL). The size and structure of nanoparticles were obtained from (XRD) and found to be 13nm and cubic structure. The results from (TEM) and (SEM) showed agglomeration of particles and it in nano size. Strong peak at 296nm appeared when using UV-Vis while six emission peaks showed from PL spectrum. The dielectric properties of nanoparticles were studied for different frequency and showed a decrease it with increased frequency.

Keywords: PL spectrum, Nanoparticles, Photolysis, Emission peaks**.**

Introduction

Nanotechnology has a diversity of implementations in our daily life due to several physical and chemical properties and this back to the high surface-to-volume ratio. Cerium oxide is a semiconductor with huge exaction binding and broadband gap energy (3.19 eV) [1], that used for a great range of applications like biosensors [2], drug delivery [3], electronics [4], medical field [5], and agriculture [6]. Individual spectral properties like lattice expansion, the blue shift in ultraviolet absorption spectra [7], Raman-allowed modes shifting [8] and catalytic applications like an oxygen ion conductor in fuel cells [9], exhaust-gas conversion [10], and gas sensors [11] have been reported. With such a diversity of applications, different forms (mesoporous membrane/film or composite membrane/ film particle) of cerium oxide nanoparticles have been suggested and resolved. Particularly, the nanoparticles of cerium oxide have been greatly used due to the significant size-induced property changes [12]. Largely, the nanoparticles of cerium oxide could be prepared by chemical, physical, and biological methods [13–21]. For the time being, the photolysis method shows more advantages such as a less time-consuming process, commercial production, cost effectiveness, and large-scale. According to this method, many transitions of electrons occur inside the complex or salt of cerium causes the change in oxidation state and the mechanism of photolysis for the cerium source different according to the solvent that uses. When uses non polar solvent such as (C_6H_6, $CHCl_3$), the mechanism of photolysis as follows:

$$[M\text{-}L]\ X + h\nu \xrightarrow[365\ nm]{} [M\text{-}L\text{-}X]^{*} \xrightarrow[excited]{} M\text{-}L + X^{\bullet}$$

While, the mechanism was following exaction state when using polar solvent (THF, DMSO) as following:

$$[\{M\text{-}L\}^{+}X^{-} \leftrightarrow [M^{-\delta+}L] \xrightarrow{365\ nm} [M^{-\delta+}L] \leftrightarrow [\{M\text{-}L\}^{+}X]^{*} \longrightarrow M\text{-}L + X^{\bullet}$$

Experimental

Analytical procedure

The nanoparticles of cerium oxide were fabricated by photolysis method using the system of irradiation that is shown in Fig. 1. Firstly, (10gm) of ammonium cerium nitrate (Sigma Aldrich, USA, 99 %) were dissolved in 100ml distilled water with stirring. Then, it irradiated for two hours using irradiation cooling systems to avoid high temperature until a brown precipitate appears. The precipitated powder was filtered and washed for several times using acetone and ethanol solvents. Finally, the precipitate was sonicated for 10min and burned until a yellow precipitate of cerium oxide appears. The formation process of nanoparticles followed the following equations:

*Corresponding author e-mail: zaidhamid@sciences.uodiyala.edu.iq
DOI: 10.21608/ejchem.2018.4013.1352

[22]

$$(NH_4)_2Ce(NO_3)_6 \rightarrow Ce^{+3}$$

$$Ce^{+3} + 3OH \rightarrow Ce(OH)_3$$

Calcined it at 400C

$$Ce(OH)_3 + \frac{1}{2} O_2 \rightarrow 2CeO_2 + 3H_2O$$

Characterization

The analysis of X-ray diffraction (XRD) was recorded on a Shimadzu-XRD-6000 diffract meter, with Cu Ka radiation at 40 KV. The diffraction peaks of the of cerium oxide nanoparticle were paralleled with those of standard compounds declared in the JCPDS Date File. The analysis of transmission electron microscopy (TEM) was carried out on a Philips Tecnai G20 microscope, operating at 200 kW, while the studies of Scanning Electron Microscopy (SEM) were completed on JEOL, JSM- 67001. The spectral properties CeO_2 NPs were characterized by UV–Vis spectroscopy (Shimadzu, V-650) in the wavelengths ranging from 200 to 80nm while the dielectric constant of CeO_2 NPs was shown at different temperature in the frequency range of 50 Hz to 5 MHz using a HIOKI 3532-50 LCR HITESTER.

Results and Discussion

The identification structural for CeO_2 NPs was recorded using XRD in the range of angle 2θ between 20◦ and 80◦ as shown in Fig. 2. The good peaks at (111), (200), (220), (311), (222), (400), (331), and (422) appeared and in agreement with standard data (JCPDS card no: 89-8436). From the results, the cubic structure of CeO_2 appeared and the broadened peak obtained that the size of

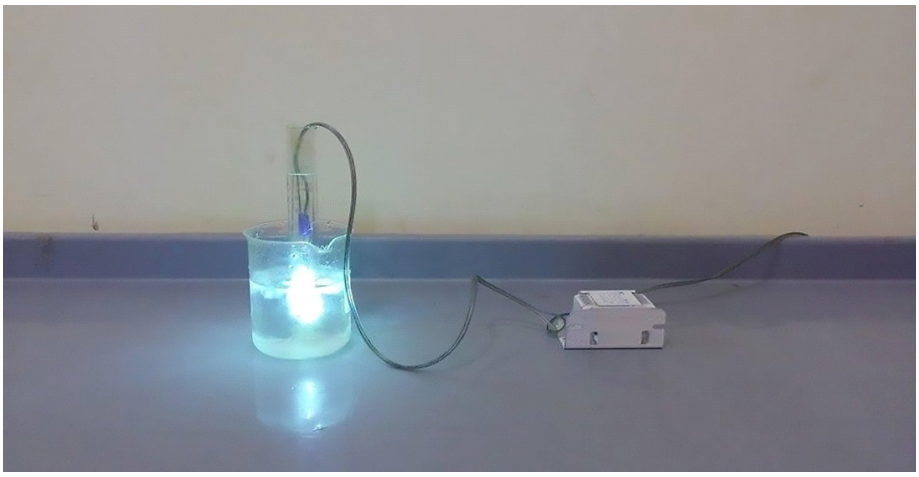

Fig. 1. System of irradiation.

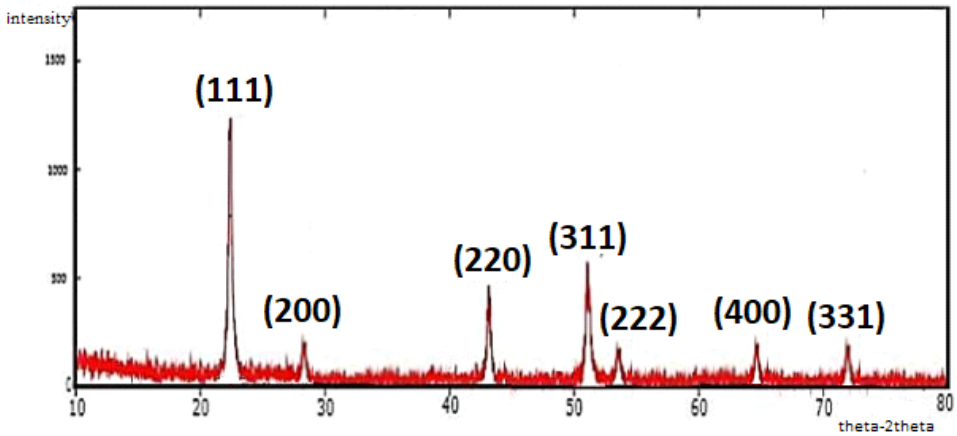

Fig. 2. XRD spectrum of CeO_2.

crystals in nanometer. The size of particles was calculated using the Scherrer formula [23] as following:

$$D = \frac{0.9\lambda}{\beta Cos\theta}$$

And the results obtained that the size of particles is 13nm.

The XPS spectrum of the oxide illustrated in Fig.3. Two peaks located at 916 and 897 eV assigned to Ce^{+4} $3d_{3/2}$ and Ce^{+4} $3d_{5/2}$ respectively,

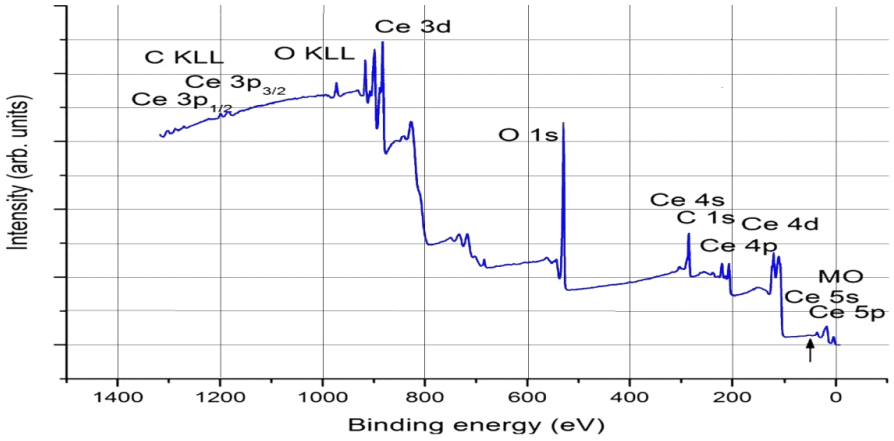

Fig. 3. XPS spectrum of CeO_2.

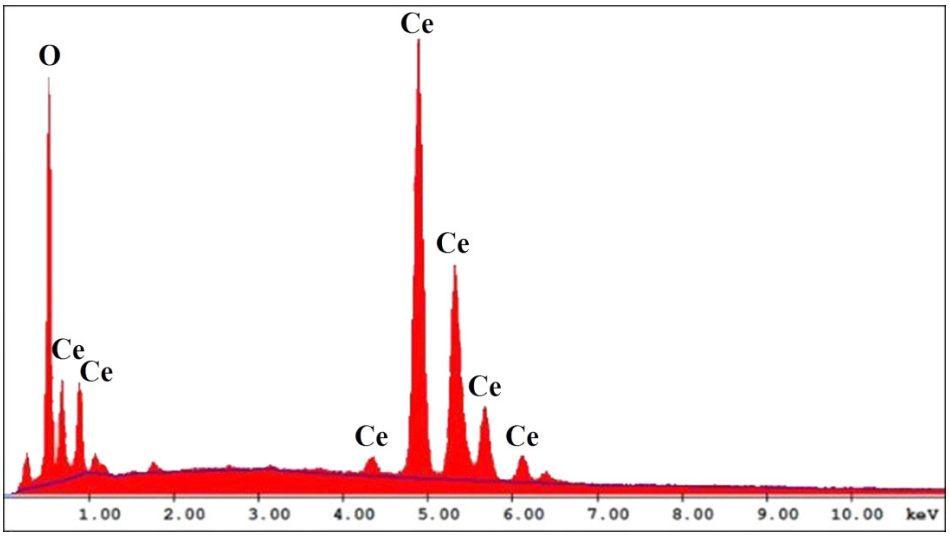

Fig. 4. EDXS spectrum of CeO_2.

while the peaks appeared at 901 and 882 eV back to trivalent state and this means finding two valence state (+4 and +3) in cerium oxide prepared.

The EDXS spectrum of nano synthesized shows that the particles contain just from Ce and O without any impurities as shown in Fig. 4.

The nanoparticles of CeO_2 NPs were undergone to the UV–vis spectrum analysis over the range of (200 to 800nm) continuously. As shown in Fig. 5, one absorption peak appeared at 297 nm which suggests that the CeO_2 NPs have an optical property and the peak that observed at 297 nm harmonizes to the structure of fluorite cubic for CeO_2 NPs due to the quantum size effect of the

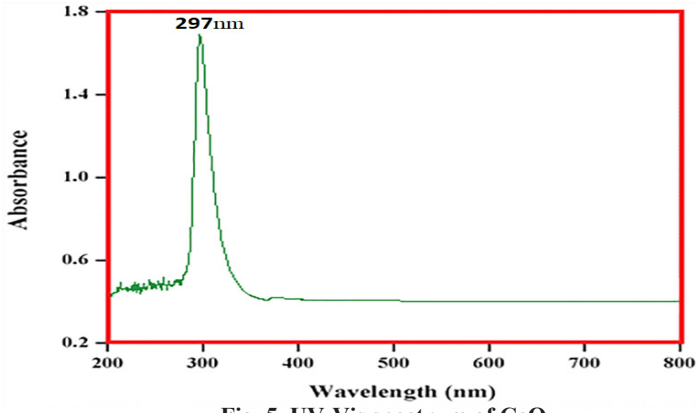

Fig. 5. UV-Vis spectrum of CeO_2.

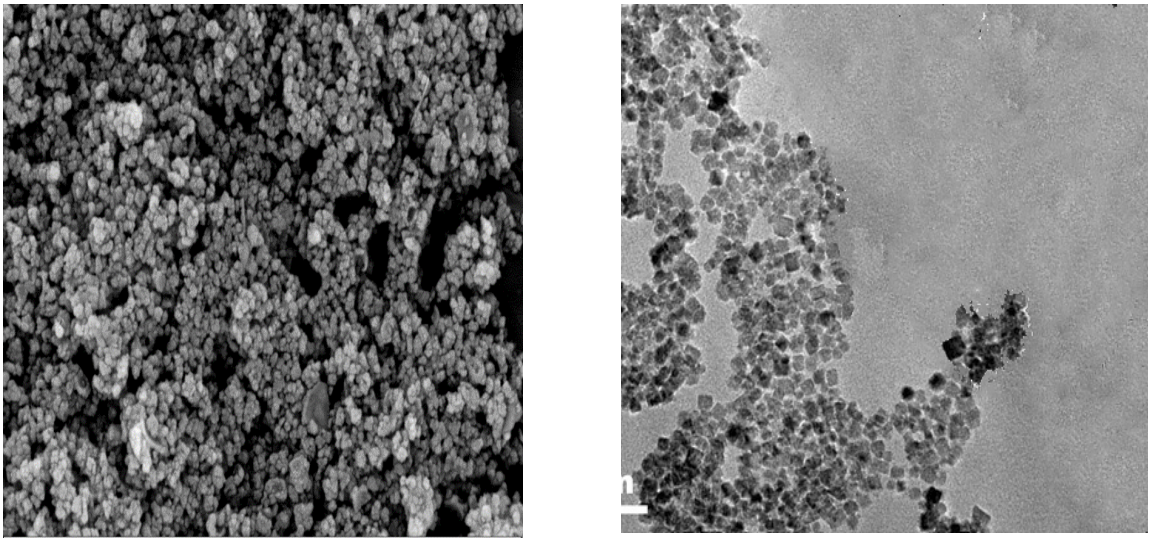

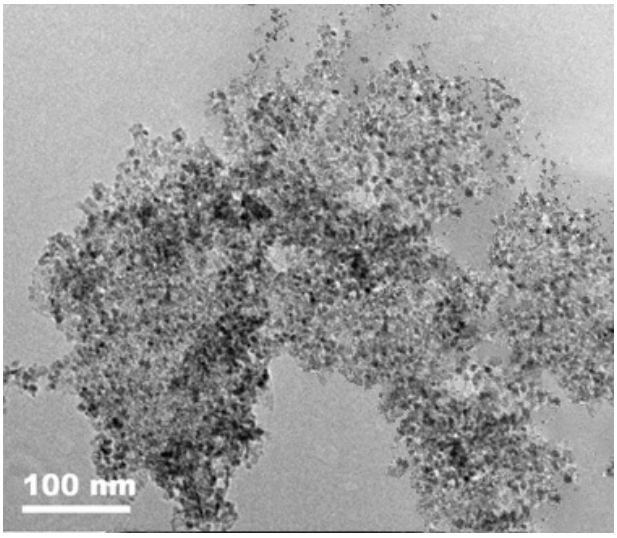

Fig. 6. TEM images of CeO_2.

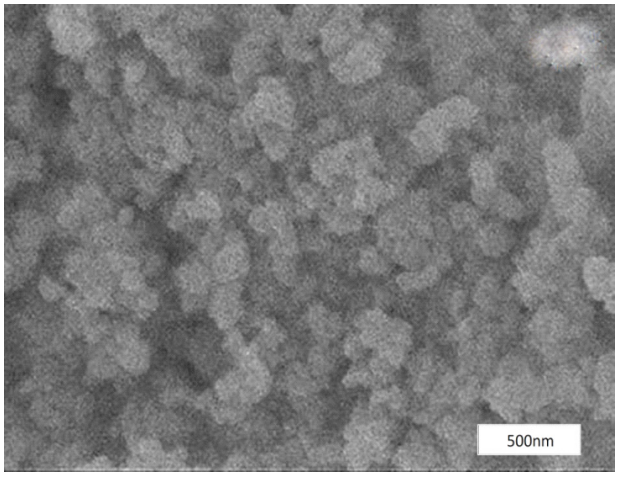

Fig.7. SEM image of CeO_2.

blue shift and confirms the charge between the O^{-2} and Ce^{+4} [3, 14].

The images of TEM for CeO_2 NPs that fabricated photolysis showed in Fig. 6. From the images, the nanoparticles of CeO_2 appeared as an agglomerated and not exactly spherical and the average is about 12nm, which is in agreement with results of XRD analysis, while the morphology of oxide provided using SEM and the results emphasize agreement with TEM about the agglomeration of particles as shown in Fig.7.

The Photoluminescence spectrum of CeO_2 NPs determined using a Xe laser of 290nm as shown Fig.8. Six emission for CeO_2 appeared; at 492nm appeared weak blue-green band, a broad band at 395nm while four blue bands appeared in

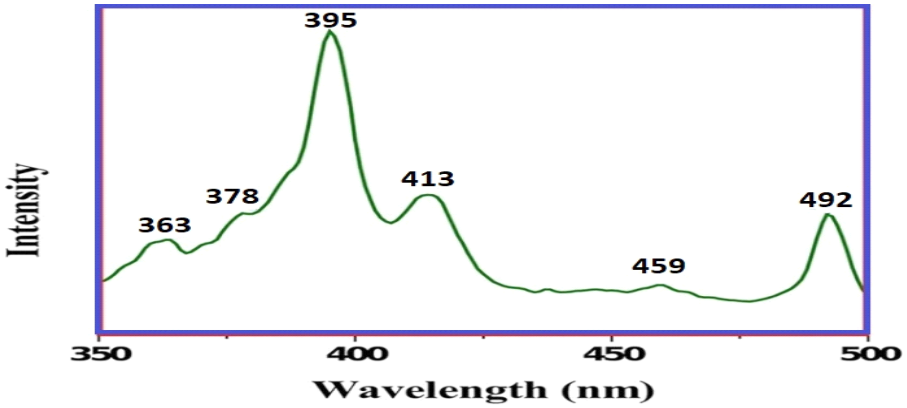

Fig. 8. PL spectrum of CeO_2.

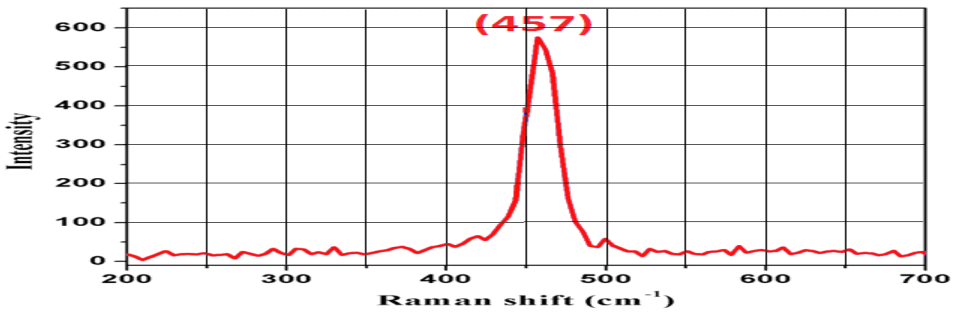

Fig. 9. Raman spectrum of CeO_2.

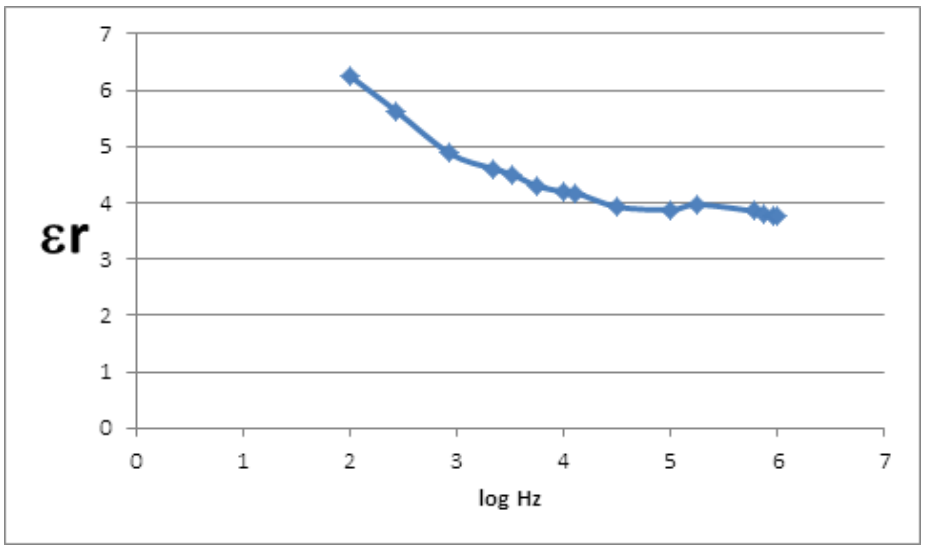

Fig. 10. Dielectric constant with log frequency

363, 378, 413, and 459 nm due to the transition of charge from the 4f band to the valence band. The weak blue-green color appeared due to surface defects in CeO_2 NPs and because of the low density of oxygen vacancies, the intensity of the green emission peak was low [15].

The spectrum of Raman showed in Fig.9. The results appeared two peaks centered at 458 and 461cm^{-1} assigned to CeO2 nanoparticles. At 457cm^{-1}, sharp Raman peak observed, which is back to Ce-O symmetrical stretching.

The constant of the dielectric and the dielectric loss of the pellets of CeO_2 NPs in disk form were determined at different temperatures and frequencies. By using the following relation, the constant of the dielectric was evaluated.

$$\varepsilon_r = \frac{Cd}{\varepsilon_0 A}$$

Where A: the area of the sample while d is the thickness.

As Fig. 10, the difference of temperature and frequency with the dielectric constant for CeO_2 NPS appeared. At low frequencies, the dielectric constant (ε_r) of CeO_2 NPs is high and reduce rapidly with the utilized frequency at all temperatures due to the effect increase ion jump orientation and the increased space charge effect. In presence of space charge, the field inside a dielectric modified and this leads to high field intensity at the certain location causing the formation of voids and these voids lead to increase in the electric field in the nearby region. Most the nanomaterial reside in the grain boundaries, which become electrically effective due to the charge trapping. At low frequencies, the dipole moment can easily pursue the changes in the electric field. Hence, the contributions to the constant of dielectric increases out of space charge polarization and rotation polarization, which take place mainly in interfaces [24].

Conclusion

The nanoparticles of cerium oxide have been successfully prepared using photolysis method. The itemized characterization study showed the formation of cerium oxide nanoparticles cubic structure and an agglomeration morphology with the average size of 13 mm. The dielectric constant of cerium oxide NPs increased firstly, but when applied frequency, it decreased.

References

1. Zaid, H. Synthesis of Bismuth oxide Nano powders via electrolysis method and study the effect of change voltage on the size for it. *Australian Journal of Basic and Applied Sciences*, **11**(7), 97-101 (2017).

2. Zaid, H.; Aklasahmed, A. Removal of Pb+2 ions from Water by Magnetic Iron Oxide Nanoparticles that Prepared via ECD. *European Journal of Scientific Research,* **145**, 354–365 (2017).

3. Patil, S.; Sandberg, A.; Heckert, E.; Self, W.; Seal, S. Protein adsorption and cellular uptake of cerium oxide nanoparticles as a function of zeta potential. *Biomaterials*, **28**, 4600–4607 (2007).

4. Thakur, S.; Patil, P. Rapid synthesis of cerium oxide nanoparticles with superior humidity-sensing performance. *Sens. Actuator B.,* **194**, 260–268 (2014).

5. Thill, A.; Zeyons, O.; Spalla, O.; Chauvat, F.; Rose, J.; Auffan, M.; Flank, A. Cytotoxicity of CeO_2 nanoparticles for Escherichia coli. Physico-chemical insight of the cytotoxicity mechanism. *Environ. Sci. Technol.*, **40,** 6151–6156 (2006).

6. Zhang, P.; Ma, Y.; Zhang, Z.; He, X.; Zhang, J.; Guo, Z.; Tai, R.; Zhao, Y.; Chai, Z. Biotransformation of ceria nanoparticles in cucumber plants. *ACS Nano.*, **11,** 9943–9950 (2012).

7. Kamruddin, M.; Ajikumar, P.; Nithya, R.; Raj, T. Synthesis of nanocrystalline ceria by thermal decomposition and soft chemistry methods. *Scripta Materialia*, **50**(4), 417-422 (2004).

8. Goharshadi, E.; Sara, S. Effects of different precursors on size and optical properties of ceria nanoparticles prepared by microwave-assisted method. *Materials Research Bulletin*, **47**(4), 1089-1095 (2012).

9. Lin, H. Production, Application and Market of Cerium Oxide. *Hydrometallurgy of China*, **24,** 9-11 (2005).

10. Tsai, M. Formation of nanocrystalline cerium oxide and crystal growth. *Journal of Crystal Growth*, **274**(3-4), 632-637 (2005).

11. Fu, Q.; Saltsburg, H.; Flytzani-Stephanopoulos, M. Active nonmetallic Au and Pt species on ceria-based water-gas shift catalysts. *Science*, **301**(5635), 935-938 (2003).

12. Panahi-Kalamuei, M.; Alizadeh, S.; Mousavi-Kamazani, M.; Salavati-Niasari, M. Synthesis and characterization of CeO2 nanoparticles via hydrothermal route. *J. Ind. Eng. Chem.*, **21,** 1301–1305 (2015).

13. Wijdan, A.; Zaid, H. Synthesis and Characterization of New Fe-Complex and Its Nanoparticle Oxide Using the Novel Photolysis Method. *International Journal of Pharmaceutical and Phytopharmacological Research*, **8,** 57–61. (2018).

14. Zaid, H.M; Nuha, F.A.; Aklas, A.A. Effect of Solvent on Size of Copper Oxide Nanoparticles Fabricated using Photolysis Method. *Asian Journal of Chemistry*, **30,** 223–225 (2018).

15. Soren, S.; Bessoi, M.; Parhi, P. A rapid microwave initiated polyol synthesis of cerium oxide nanoparticles using different cerium precursors. *Ceram. Int.*, **41,** 8114–8118 (2015).

16. Darroudi, M.; Hakimi, M.; Sarani, M.; Kazemi Oskuee, R.; Khorsand Zak, A.; Gholami, L. Facile synthesis, characterization, and evaluation of neurotoxicity effect of cerium oxide nanoparticles. *Ceram. Int.,* **39,** 6917–6921 (2013).

17. Yao, S.; Xie, Z. Deagglomeration treatment in the synthesis of doped-ceria nanoparticles via coprecipitation route. *J. Mater. Process. Technol.*, **186,** 54–59 (2007).

18. Darroudi, M.; Hoseini, S.J.; Oskuee, R.K.; Hosseini, H.A.; Gholami, L.; Gerayli, S. Food-directed synthesis of cerium oxide nanoparticles and their neurotoxicity effects. *Ceram. Int.*, **40,** 7425–7430 (2014).

19. Maensiri, S.; Masingboon, C.; Laokul, P.; Jareonboon, W.; Promarak, V.; Anderson, P.L.; Seraphin, S. Egg white synthesis and photoluminescence of platelike clusters of CeO_2 nanoparticles. *Cryst. Growth Des.*, **7,** 950–955 (2007).

20. Maensiri, S.; Labuayai, S.; Laokul, P.; Klinkaewnarong, J.; Swatsitang, E. Structure and optical properties of CeO_2 nanoparticles prepared by using lemongrass plant extract solution. *Jpn. J. Appl. Phys.*, **53,** 06–14 (2014).

21. Zhou, XD; Huebner, W.; Anderson, HU. Room-temperature homogeneous nucleation synthesis and thermal stability of nanometer single crystal CeO_2. *Appl Phys Lett.*, **80,** 3814 (2002)

22. Gopinath, K.; Arumugam, A. Extracellular mycosynthesis of gold nanoparticles using Fusarium solani. *Appl. Nanosci.*, **4,** 657–662 (2014).

23. Suresh, S.; Arunseshan, C. Dielectric Properties of Cadmium Selenide (CdSe) Nanoparticles synthesized by solvothermal method. *Applied Nanoscience*, **4**(2), 179–184 (2014).

24. Suresh, S. Studies on the dielectric properties of CdS nanoparticles. *Applied Nanoscience*, **4,** 325-329 (2014).

(*Received* 1/6/2018;
accepted 10/9/2018)

تحضير الضوئي لأوكسيد السيريوم النانوي من ملحه مع دراسة خواصه التركيبية والطيفية

زيد حميد محمود، اميمة عماد خلف، محمد علوان فرحان
قسم الكيمياء - كلية العلوم - جامعة ديالى - العراق.

حضرت دقائق اوكسيد السيريوم النانوية بأستخدام طريقة التحلل الضوئي الجديدة .وتم تشخيص الدقائق باستخدام تقنية حيود الاشعة السينية، مطيافية الاشعة فوق البنفسجية، المجهر الالكتروني النافذ، المجهر الالكتروني الماسح، اطياف رمان، اطياف الاشعة السينية الالكتروضوئية. بينت حجم وتركيب الدقائق النانوية من حيود الاشعة السينية ووجد ان حجمها هو 13 نانومتر وذات شكل مكعب. النتائج من المجهرالالكتروني الماسح والنافذ اظهرت تجمعات من الدقائق في الحجم النانوي. قمة قوية عند طول موجي 296 نانومتر ظهرت باستخدام مطيافية الاشعة الفوق البنفسجية بينما ظهرت ستة قمم انبعاث باستخدام تقنية .PL درست الخصائص الكهربائية للدقائق النانوية في ترددات مختلفة ووجد بانها تقل بزيادة التردد.